Geophysical Prospecting

EAGE EUROPEAN ASSOCIATION OF GEOSCIENTISTS & ENGINEERS

Geophysical Prospecting, 2010, 58, 229–234 doi: 10.1111/j.1365-2478.2009.00820.x

Feasibility of joint 1D velocity model and event location inversion by the Neighbourhood algorithm

Jaromir Jansky[1], Vladimir Plicka[1]* and Leo Eisner[2‡]

[1]*Department of Geophysics, Faculty of Mathematics and Physics, Charles University in Prague, V Holešovičkách 2, 180 00 Prague 8, Czech Republic, and* [2]*Microseismic Inc., 800 Tully Road, Suite 175, Houston, TX 77079, USA*

Received November 2008, revision accepted June 2009

ABSTRACT

Using a set of synthetic P- and S-wave onsets, computed in a 1D medium model from sources that mimic a distribution of microseismic events induced by hydrofrac treatment to a monitoring geophone array(s), we test the possibility to invert back jointly the model and events location. We use the Neighbourhood algorithm for data inversion to account for non-linear effects of velocity model and grid search for event location. The velocity model used is composed of homogeneous layers, derived from sonic logging. Results for the case of one and two monitoring wells are compared. These results show that the velocity model can be obtained in the case of two monitoring wells, if they have optimal relative position. The use of one monitoring well fails due to the trade-off between the velocity model and event locations.

INTRODUCTION

Hydraulic fracture treatments in oil and gas reservoirs are often used to stimulate the production by injecting fluids under pressure high enough to fracture the formation and create conductive paths in the reservoir. Such treatments induce microseismic activity that can be monitored by geophone array(s) deployed in nearby monitoring well(s). The arrival time of *P*- and *S*-waves and their polarization data can be used to determine the hypocentral locations of these events, if a suitable velocity model of the medium is known.

The velocity model is often obtained from sonic logging that estimates the velocity from signals that propagate in the vertical direction and at a frequency up to 20 thousands of Hz. However, seismic waves between induced seismic events and monitoring borehole propagate mainly in the horizontal direction and at significantly lower frequencies (below 500 Hz). In the case of anisotropy the rays from induced microseismic events may propagate by slightly different velocity. This study investigates the possibility to estimate the medium model by an independent approach, using joint inversion for hypocentral locations and the velocity model. If such inversion would be feasible and accurate it could be used to improve the velocity model and location accuracy.

Joint velocity model estimation and hypocentral localizations are frequently used in earthquake seismology with good distribution of the receivers and earthquakes (e.g., Hauksson and Haase 1997). However, such inversions are relatively rare in studies of induced seismic activity because of the limited distribution of the receivers and induced events (e.g., Charléty *et al.* 2005).

In this study we investigate such a possibility by the inversion of synthetic traveltimes computed in a 1D velocity model composed of homogeneous layers for one and two monitoring nearly vertical arrays of receivers. The investigation of a 1D structure is justified by two sonic logs in two nearby boreholes. This model was constructed from the slowness averaging of sonic log data of one gas field in West Texas (Vavryčuk, pers. comm.; Bulant and Klimeš 2008). This model (M0) is shown in Fig. 1.

*E-mail: vp@karel.troja.mff.cuni.cz

‡Formerly at Schlumberger Cambridge Research, High Cross, Madingley Road, Cambridge CB3 0EL, UK

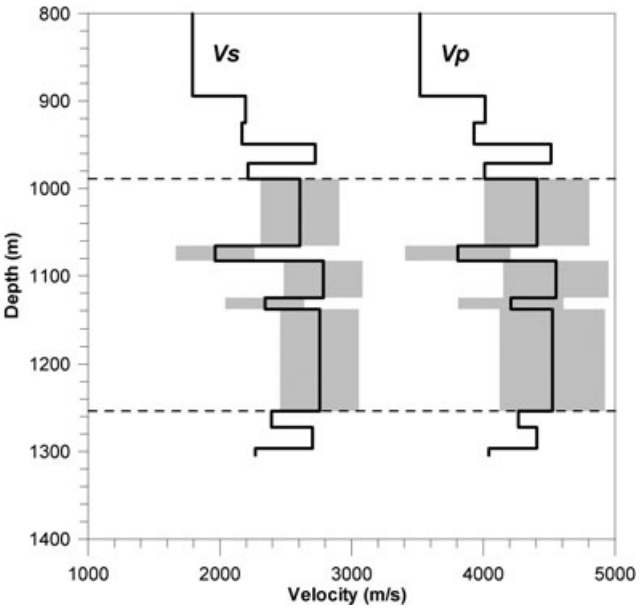

Figure 1 Model M0. Only the portion of the model below the depth of 800 m is shown. In the upper part of the model the velocities do not change. The shaded area shows the velocity range in which the model from data inversion is looked for by the Neighbourhood algorithm.

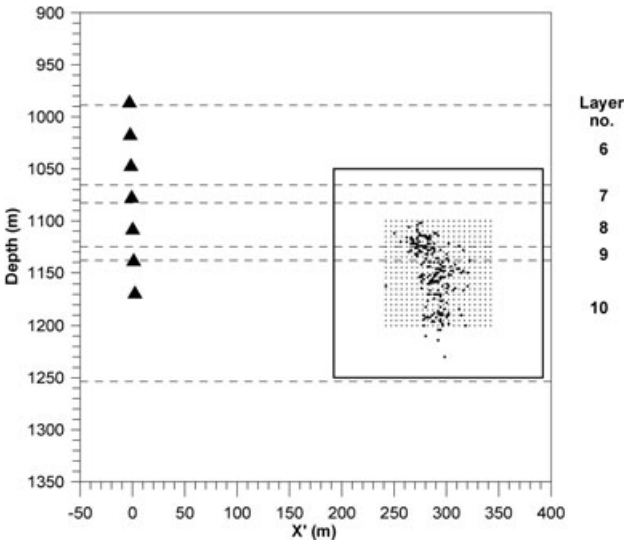

Figure 2 Depth distribution of geophones (triangles) and depth and epicentral distance distribution of 449 strong real events (heavy dots), located in model M0 by grid search. The small crosses mark the distribution of 441 synthetic events. The square shows the area in which the location of events is searched for during the data inversion. Dashed horizontal lines show layer boundaries as derived from the sonic logging.

Many different techniques can be used to derive a structural model from arrival times. We have selected the Neighbourhood algorithm method (Sambridge 1999), because in highly non-linear space, such as joint inversion of velocity and location, it has more 'power' to escape from local minima than, for example, genetic algorithms (Sambridge 1999; Valleé and Bouchon 2004) or even least squares (Leaney 2008).

The thickness of the homogeneous layers was set equal to the thickness determined from the sonic log because the lithological boundaries are well detected in the sonic logging. Thus, with these boundaries we reduced the non-linearity of the inversion by searching just for velocity values in these layers. The 1D velocity model is estimated only in the depth range from 989–1253 m (see Fig. 1), where the seismic rays from sources to receivers sample the medium (distribution of receivers and sources in Fig. 2). These depths coincide with the depth of the bottom of the 5th and 10th layer of the 13 layers in model M0.

First, we have carried out a limited number of inversions to obtain the optimal parameters for the NA inversion (i.e., number of iterations, number of models generated in each iteration, limits on area in which the locations are looked for by grid search, etc.). In the inversion procedure (see flowchart in Fig. 3) we have used 80 initial models and generated 80 models during 401 iterations. Consequently, a total of 32 080 reser-

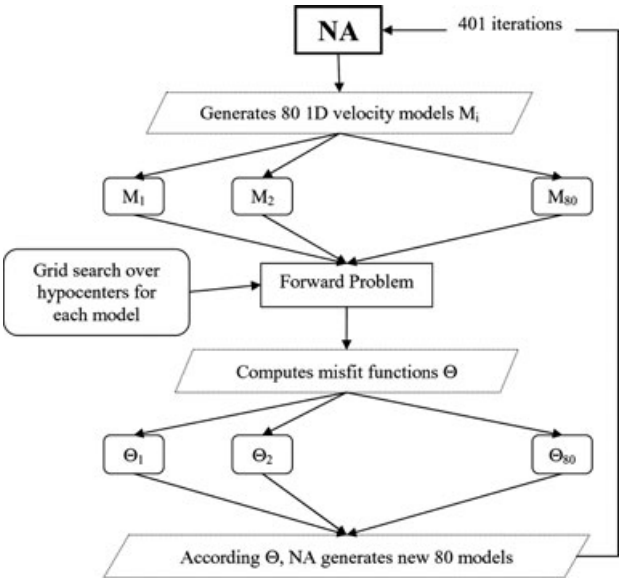

Figure 3 Flowchart of joint inversion of the velocity model and event location using the Neighbourhood algorithm (NA) and grid search.

voir models were generated by the Neighbourhood algorithm. The number of iterations and number of models in iteration was chosen to ensure the stability of convergence of the misfit function to its minimum. The lower and upper boundaries on velocities are estimated so that the resulting model lies well

inside them. To measure the quality of the inversion we define the normalized misfit function Θ as follows:

$$\Theta = \frac{1}{N}\sum_{i=1}^{E}\sum_{k=1}^{S}\left(|r_{ijk}^{P}| + |r_{ijk}^{S}|\right), \qquad N = ES. \tag{1}$$

Here E is number of events, S is number of stations and r_{ijk}^{P}, r_{ijk}^{S} are traveltime residuals for P- and S- waves, respectively for i-th event at k-th station from j-th inverted position. To find the proper Θ for each event we have to go through all hypocentres tested in inversion to find the hypocentre j with minimal sum of traveltime residua for all stations.

For each individual event i traveltime residue for P- and S-waves, r_{ijk} is defined by the given velocity model, generated by the Neighbourhood algorithm (V_P and V_S) for a given point of source grid j and receiver k:

$$r_{ijk} = A_{ijk} - H_{ij} - T_{ijk},$$

where A_{ijk} is traveltime for the inverted model, H_{ij} is origin time for i event at j grid and T_{ijk} is traveltime for true model (which would be picked arrival times in a real data set). Finally, origin time is found for each model by averaging from arrival times:

$$H_{ij} = \frac{1}{S}\sum_{k=1}^{S}(A_{ijk} - T_{ijk}). \tag{2}$$

THE CASE OF ONE MONITORING WELL

For microseismicity, monitored from a single vertical array of receivers, only the epicentral distance from receivers and the depth can be estimated from arrival times, while the final epicentres are determined from particle polarization (House 1987; Fischer *et al.* 2008). We therefore deal in this chapter only with the epicentral distances and depths. In this study we test one monitoring well geometry mimicking the situation of the Canyon Sand field (Fischer *et al.* 2008). Figure 2 shows the geophones and location of 449 real microseismic events induced by the hydraulic fracturing. The events were located from real picks by the grid search method in model M0, using the step of 2 m in both epicentral and vertical directions.

The synthetic traveltime data are computed for a set of 441 synthetic events that are distributed regularly in epicentral distance (21 epicentral distances) and depth (21 depths) with the step of 5 m so that they cover the epicentral distance and

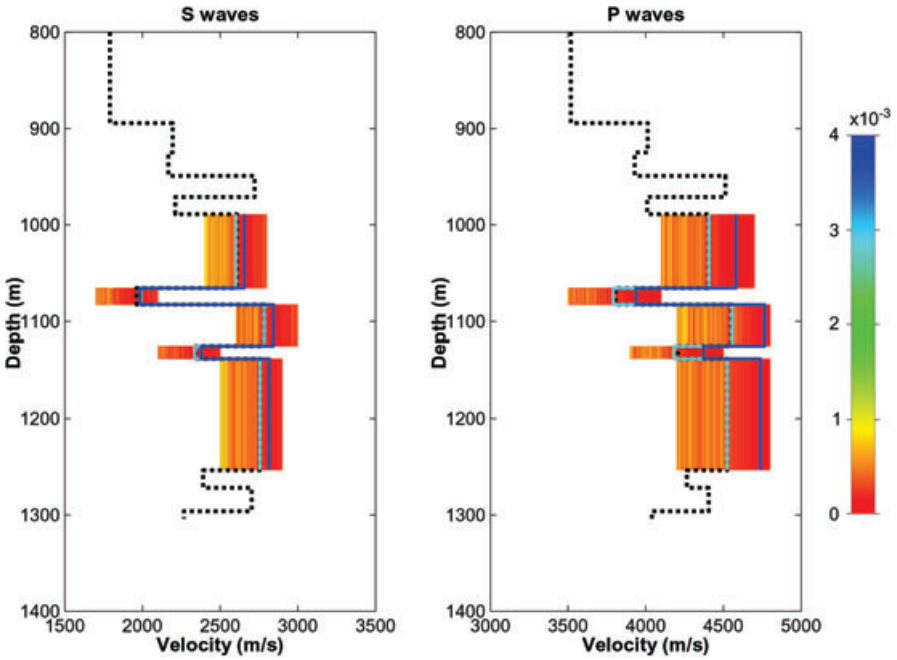

Figure 4 Velocity model M0 (dashed line) and individual velocity models obtained during the inversion of synthetic data, with the normalized misfit function given by colour. The best model, M1, is shown by blue bold line. Model MF (cyan line) is obtained by inversion of data if the event positions are kept fixed.

depth area of the real data set shown in Fig. 2. The synthetic traveltimes A_{ijk} of equation (2) are computed with the accuracy of 0.1 ms, i.e., the accuracy is slightly better than the accuracy of the real resampled data. We consider that each synthetic event is recorded at each station, so we have 3087 *P*- and 3087 *S*-wave onsets. We use only 7 receivers as the 8th receiver did not provide reliable arrival time picks (poor coupling).

Inversion of the velocity model generated by the Neighbourhood algorithm is limited to the shaded area in Fig. 1. The grid search for locations is looked for in the area shown in Fig. 2, with the step of 5 m in the depth and in the epicentral distance so that this search contains the original positions of all 441 synthetic events. For each event we search 1681 positions in each generated model to find the position with the minimum misfit.

Figure 4 shows the range of velocity models obtained during the inversion of synthetic data. The colour shows the value of the normalized misfit of equation (1) of each model. In these models the structure above and below our range of depths, i.e., 989–1253 m respectively, is identical with the model M0. The best model, M1, is shown by a blue bold line. Model M0 (black dotted line) is shown for comparison. We see a large difference between M0 and M1 and a large uncertainty in the inversion.

The deviation of M1 from M0 is significantly larger for *P*-wave velocity. This should be explained by the *P*- and *S*-wave residuals having the same weight, as was done in our study. As explained in the Appendix the *S*-wave velocity difference DV_S from the proper V_S causes the same traveltime residual (if the residual is small compared to the traveltime) as it causes the DV_P difference from the proper V_P that is roughly $DV_P \sim DV_S\ (V_P / V_S)_2$. Finally, note that the minimum of relative misfit is broad, indicating large uncertainty in the inverted model, i.e., a large number of models satisfies arrivals at the single monitoring well.

Thus, we conclude that the search of the model fails in our example of one monitoring well, even in the case of inversion of accurate synthetic data. It is due to the trade-off between the model and events position. The location of all synthetic events in M1 is namely shifted in epicentral distance of one grid step (5 m) to smaller epicentral distances. In this geometry the depths are not affected by the trade-off. To confirm this, we ran the inversion of the data using fixed events position. In this case, we obtain from the inversion a model MF (cyan line in Fig. 4) that is practically identical with M0. A small difference can be observed only in layer 9 for V_P and in layer 7 for V_S. These layers are thin, weakly sampled by the rays.

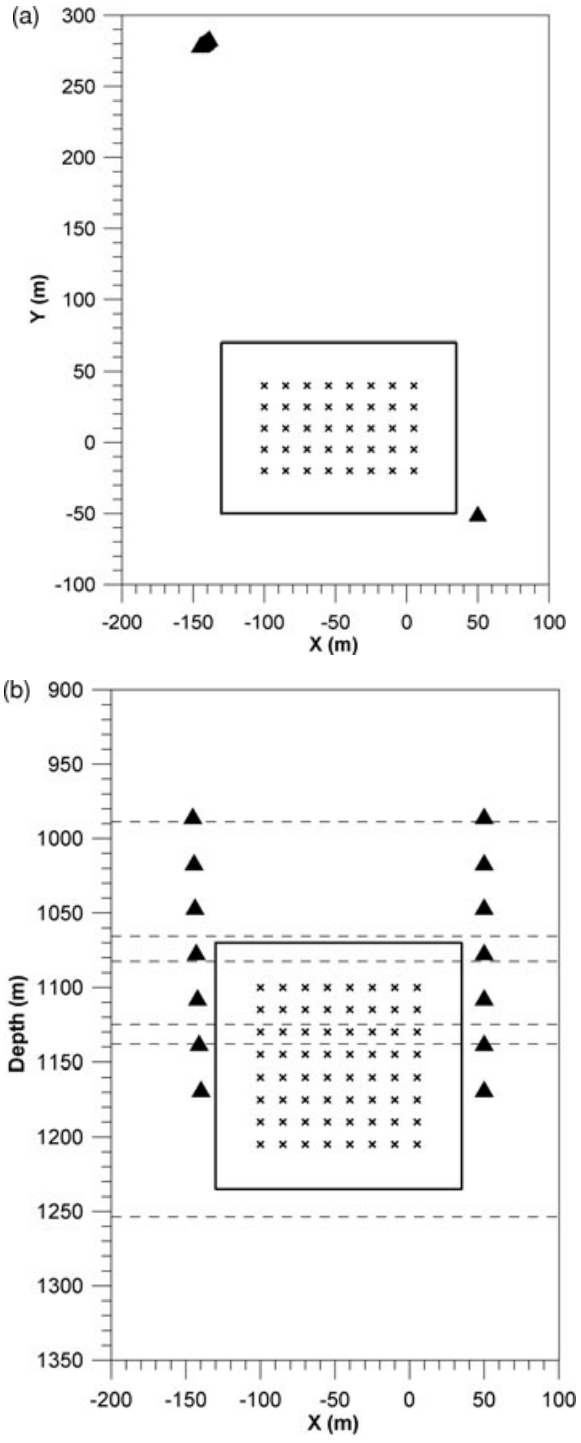

Figure 5 a) The map view of the geophones distributed in two monitoring wells (triangles) and a set of 320 synthetic hypocentres (crosses). Forty events (5 × 8) are distributed in each of the 8 depths' levels. The step in both horizontal directions and in the depth equals 15 m. The location of the hypocentres in the best model M3D (see Fig. 6) are identical with their original position. B) as in a) but for XZ vertical cross-section.

The results of the inversion are to a certain extent sensitive to the chosen inversion parameters. Therefore the regular shift in location for 1-well (as shown) is just accidental. In other cases the shift can be more random but generally not chaotic. For example, the compact part of the hypocentres is shifted by two grids and the other compact part just by one grid. The real data are certainly not so homogeneous, as are our synthetic data. In our computation we did not take into consideration possible uncertainties in receiver position resulting from deviation surveys that can have an order of magnitude larger effects, as illustrated by Bulant *et al.* (2007).

THE CASE OF TWO MONITORING WELLS

For microseismicity monitored from two vertical arrays of receivers, the full hypocentral location can almost be inverted using only arrival times. We test joint velocity and location inversion for two monitoring wells by adding the second monitoring well to the first well in a way that mimics the situation of the Cartage Cotton Valley gas field (Rutledge and Phillips 2003). Figure 5(a) shows the map view and Fig. 5(b) the XZ vertical cross-section of the distribution of geophones in two monitoring wells and 320 synthetic hypocentres. Forty events (8×5) are distributed in each of the 8 depth levels. The step in both horizontal directions and in the depth equals 15 m. The synthetic hypocentres therefore regularly cover a cube with dimensions of $105 \times 60 \times 105$ m.

We have used 4480 *P*- and 4480 *S*-wave onsets (we have, in fact just 14 receivers, see remark above). These synthetic data are then inverted so that the velocity generated by the Neighbourhood algorithm, as in Chapter 1, is again limited to the shaded area in Fig. 1. The grid search for location is for each event looked for in the cube whose limits are given by squares in Figs 5(a) and 5(b). The grid step in both horizontal directions and in the depth equals 5 m. For each event and model we search 15 028 positions. This grid is defined so that it contains the original positions of all the 320 synthetic events.

Figure 6 shows all the models obtained during the inversion coloured by their corresponding misfit function (equation (1)). The best model M3D obtained from the inversion practically does not differ from M0. A small difference can be observed only in the layer 9 for V_P. This is again a thin layer only weakly sampled by the rays. The minimum of relative misfit is narrower than in the case of one monitoring well indicating lower uncertainty in the inverted model. The location of synthetic events in model M3D agrees exactly with their original positions.

The geometrical configuration of the two monitoring wells used in this study represents a case suitable for velocity model

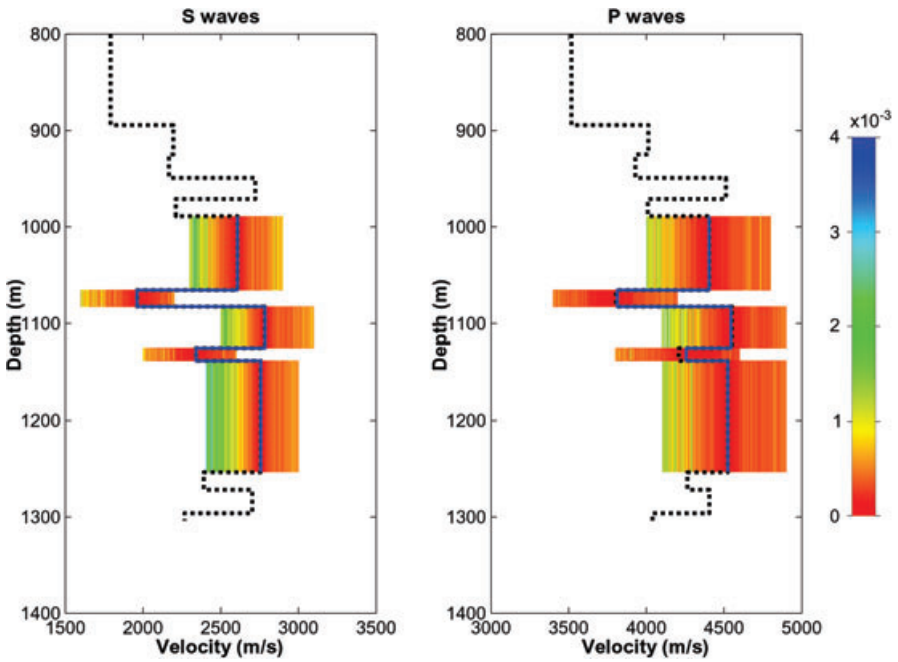

Figure 6 Velocity model M0 (dashed line) and individual velocity models obtained during the inversion of synthetic data in the case of two monitoring wells, with the normalized misfit function given by colour. The best model, M3D, is shown by blue bold line.

inversion. Several tests that used another position of the second monitoring well resulted in velocity models that differed more from the M0 model and as well the location of the synthetic events were shifted from their original position. All these differences depend significantly on the relative geometrical position of the monitoring wells and the located events. Thus, we recommend carrying out a synthetic test before inverting real data for particular geometry.

CONCLUSIONS

Our synthetic test shows that independent estimation of velocity-depth distribution in an area of induced microseismic events, using joint model estimation and hypocentre location, is possible only in the case of using at least two monitoring wells with suitable positions relative to the area of located events, even in the case of a simple 1D velocity model composed of homogeneous layers. The use of only one monitoring well fails due to the trade-off between the model and hypocentre location. Real data are far less homogeneous (different accuracy of phase readings) and regular (not equally spaced through the inversion model) than synthetic data, so the results of inversion should be expected to be less accurate.

ACKNOWLEDGEMENTS

We thank James T. Rutledge for making the phase reading sets available. We thank also other colleagues participating in the IMAGES project for their help. We thank Dominion Exploration Company for releasing the data set used in this study. We acknowledge the European Union for funding the IMAGES Transfer of Knowledge project (MTKI-CT-2004-517242). This work was also partially supported by the MSM0021620860 and GACR-205–07-0502 grants in the Czech Republic.

REFERENCES

Bulant P., Eisner L., Pšenčík I. and Le Calvez J. 2007. Importance of borehole deviation surveys for monitoring of hydraulic fracturing treatments. *Geophysical Prospecting* **55**, 891–899.

Bulant P. and Klimeš L. 2008. Comparison of VSP and sonic log data in non-vertical wells in a heterogeneous structure. *Geophysics* **73**, U19–U25.

Charléty J., Cuenot N., Dorbath C. and Dorbath L. 2005. Four dimensional velocity structure of the Soultz-sous-Forêts geothermal reservoir during the 2000 and 2003 stimulations. *Proceedings of the 30th Workshop on Geothermal Reservoir Engineering Stanford University*, Stanford, California, 31 January–2 February 2005.

Fischer T., Hainzl S., Eisner L., Shapiro S.A. and Le Calvez J. 2008. Microseismic signatures of hydraulic fracture growth in sediment formations: Observations and modeling. *Journal of Geophysical Research* **113**, B02307. doi:10.1029/2007JB005070

Hauksson E. and Haase J.S. 1997. Three-dimensional V_p and V_p/V_s velocity models of the Los Angeles basin and central Transverse Ranges, California. *Journal of Geophysical Research* **102**, 5423–5453.

House L. 1987. Locating microearthquakes induced by hydraulic fracturing in crystalline rocks. *Geophysical Research Letters* **14**, 919–921.

Leaney W.S. 2008. Inversion of microseismic data by least-squares time reversals and waveform fitting. SEG meeting, Las Vegas, Nevada, USA, Expanded Abstracts.

Rutledge J.T. and Phillips W.S. 2003. Hydraulic stimulation of natural fractures as revealed by induced microearthquakes, Carthage Cotton Valley gas field, east Texas. *Geophysics* **68**, 441–452.

Sambridge M. 1999. Geophysical inversion with a neighbourhood algorithm. I. Searching a parameter space. *Geophysical Journal International* **138**, 479–494.

Valleé M. and Bouchon M. 2004. Imaging coseismic rupture in far field by slip patches. *Geophysical Journal International* **156**, 615–630.

APPENDIX

Let us for simplicity consider a homogenous medium characterized by V_P and V_S velocity in which we have inverted velocities V'_P and V'_S. Then $\Delta V_P = V'_P - V_P$ is the difference between the *P*-wave velocity V_P and found velocity V'_P, r the traveltime residual and X the epicentral distance. Then

$$\Delta V_P = V'_P - V_P = \frac{X}{(T_P - r)} - \frac{X}{T_P} = \frac{Xr}{(T_P - r)\,T_P}.$$

An analogous relationship can be found for *S*-wave velocity. Assuming $r \ll T_S$ and using relation $T_S = \frac{T_P V_P}{V_S}$ then

$$\frac{\Delta V_P}{\Delta V_S} = \frac{T_S\,(T_S - r)}{T_P\,(T_P - r)}$$

$$\lim_{r \to 0} \left(\frac{T_S\,(T_S - r)}{T_P\,(T_P - r)} \right) = \frac{T_S^2}{T_P^2} = \left(\frac{V_P}{V_S} \right)^2$$